Scattering Parameter Transient Analysis of Transmission Lines Loaded with Nonlinear Terminations

JOSE E. SCHUTT-AINE, STUDENT MEMBER, IEEE, AND RAJ MITTRA, FELLOW, IEEE

Abstract—**This work presents a new approach for the time-domain simulation of transients on a dispersive and lossy transmission line terminated with active devices. The method combines the scattering matrix of an arbitrary line and the nonlinear causal impedance functions at the loads to derive expressions for the signals at the near and far ends.**

The problems of line losses, dispersion, and nonlinearities are first investigated. A time-domain formulation is then proposed using the scattering matrix representation. The algorithm assumes that dispersion and loss models for the transmission lines are available and that the frequency dependence is known. Large-signal equivalent circuits for the terminations are assumed to be given. Experimental and computer-simulated results are compared for the lossless dispersionless case, and the effects of losses and dispersion are predicted.

I. INTRODUCTION

IN TODAY'S MANY applications of integrated circuits and printed circuit boards, transmission lines and interconnections play an instrumental role at virtually every level of integration. With the design of fast devices having switching times in the picosecond range, transmitting data at high megabaud rates has become very commonplace in modern digital computers and switching networks used for telecommunication. Signal delays and rise times are more and more limited by interconnection lengths rather than by device speed and represent a potential obstacle to the ultimate scaling on VLSI technology. In recent years, modeling interconnections has become a major focus of interest in the implementation of digital and microwave circuits. Shorter rise and fall times as well as higher frequency signals have compelled most transmission lines to operate within ranges where dispersion is no longer negligible. Skin effect and losses contribute to signal corruption leading to waveform attenuation as well as pulse rise and fall time degradations. In wafer-scale integration, these losses can become very significant and may lead to an *RC* type behavior of the lines. Finally, in the case of multiconductor lines, cross-coupling between neighboring lines may increase the level of distortion in excited lines which can initiate false signals in nonexcited lines.

The implementation of a high-density-compatible packaging scheme is essential for the design of high-speed digital systems such as gallium arsenide integrated circuits. For microwave or digital applications, printed circuit boards, chip carriers, and modeling of these networks represent the first step toward implementing reliable design guidelines. A complete CAD tool for studying these effects would require a frequency-domain characterization of the transmission line with higher-order modes included to account for dispersion. Numerous authors have investigated the properties of microstrip lines at high frequencies and derived expressions relating the propagation characteristics to frequency [1]–[10]. Full-wave and simplified models have been proposed to describe these effects and to derive the frequency dependence of the characteristic impedance and the propagation constant. Other geometries, such as stripline, buried microstrip, and coplanar, have thus far received less attention but obey the same restrictions imposed on the electrical performance of microstrip at microwave frequencies.

Of equal importance is the analysis of a high-speed or high-frequency signal propagating on a dispersive and lossy transmission line. Such an analysis requires a complete and accurate frequency characterization of the structure of interest and, for practicality, must implement the nonlinear and time-changing behaviors of the terminations, which are transistors, logic gates, or other types of active devices. Several investigators have attempted to set up analytical models describing wave propagation in such systems. Solutions for lossless lines with arbitrary terminations were obtained by Mohammadian *et al.* [12] using a forward and backward wave approach. Veghte and Balanis [13] have analyzed the distortion of a pulse due to dispersion along a microstrip transmission line. Caniggia [14] combined macromodels for transmission lines and terminations, and Djordjevic *et al.* [11] used a Green's function approach to simulate the time-domain transient on a multiconductor array with nonlinear terminations.

In this study, a combined frequency-domain, time-domain approach is used to formulate the propagation equations on a dispersive and lossy line with nonlinear behavior at the terminations. The novelty of the method resides in the formulation, which separates the linear expressions for the transmission line from the nonlinear expressions for the terminations by means of scattering parameters and the use of an auxiliary reference imped-

Manuscript received August 1, 1987; revised October 4, 1987.

The authors are with the Electromagnetic Communication Laboratory, Department of Electrical and Computer Engineering, University of Illinois, Urbana, IL 61801.

IEEE Log Number 8718865.

0018-9480/88/0300-0529$01.00 ©1988 IEEE

ance. A time-domain flow-graph representation of the solution is also derived. In the lossless case, the solution reduces to very simple expressions which greatly increase computational efficiency.

II. Formulation

Consider an arbitrary transmission line with arbitrary loads at both ends (see Fig. 1). The differential equations relating the voltage V and the current I along the line are expressed by

$$-\frac{\partial V}{\partial x} = L_0 \frac{\partial I}{\partial t} + R_0 I \tag{1a}$$

$$-\frac{\partial I}{\partial x} = C_0 \frac{\partial V}{\partial t} + G_0 V \tag{1b}$$

where L_0, C_0, R_0, and G_0 are the inductance, capacitance, resistance, and conductance per unit length, respectively. The solutions for time-harmonic excitation are usually written in the frequency domain as ($\omega = 2\pi f$ is angular frequency)

$$V(\omega, x) = Ae^{-\gamma x} + Be^{+\gamma x} \tag{2a}$$

$$I(\omega, x) = \frac{1}{Z_0}[Ae^{-\gamma x} - Be^{+\gamma x}] \tag{2b}$$

where

$$\gamma = \sqrt{(R_0 + j\omega L_0)(G_0 + j\omega C_0)} \qquad Z_0 = \sqrt{\frac{R_0 + j\omega L_0}{G_0 + j\omega C_0}}. \tag{3}$$

Here γ and Z_0 are complex, leading to an attenuation of the signal as it propagates through the medium. If the terminations are linear and time-invariant (i.e., $Z_1(t)$ and $Z_2(t)$ are constant with time), the coefficients A and B can be determined by matching boundary conditions at $x = 0$ and $x = l$; next, an inverse Fourier transform approach can be used to solve for the time-domain solution. On the other hand, if the terminations are nonlinear or time-changing, then the boundary conditions must be formulated in the time domain as

$$V_s(t) = V(t,0) + Z_1(t) I(t,0) \tag{4}$$

$$Z_2(t) I(t,l) = V(t,l) \tag{5}$$

where $V_s(t)$ is the source voltage. $Z_1(t)$ and $Z_2(t)$ indicate the time variations of the source and load terminations, respectively. For any time greater than t, $Z_1(t)$ and $Z_2(t)$ are not known, since they depend on the voltage and current solutions at time t. In fact, the evaluation of $Z_1(t)$ and $Z_2(t)$ may involve several iterations that involve solving the terminal network equations with trial values until convergence to the true impedance values. Transforming conditions (4) and (5) into the frequency domain is inappropriate, and a time-domain formulation is thus necessary. Likewise, (2) and (3) cannot conveniently be analytically inverted into the time domain and constrained to satisfy (4) and (5). This limitation arises not only because of the dispersive and frequency-dependent characteristics

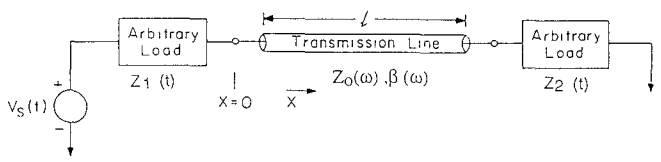

Fig. 1. Transmission line with nonlinear terminations and source generator.

of the line, but also because the evaluation of the coefficients A and B requires an *a priori* knowledge of the time-dependent load functions. A formulation in which the causality of the boundary conditions is implied thus becomes necessary. The use of scattering parameters allows one to define the properties of the transmission line independently from those of the terminations; consequently, by properly combining load and line relations, a simple expression for the solutions can be derived.

III. Scattering Parameter Formulation

Any linear two-port network can be described as a set of scattering parameters (S parameters) which relate incident and reflected voltage waves. These waves are variables which depend on the total voltages and currents at the two-port. If ideal (lossless and dispersionless) transmission lines of known characteristic (reference) impedance Z_{ref} are connected to both ports of a linear network, then the voltage waves on the reference lines (see Fig. 2) a_1, b_1, a_2, b_2 are defined as the incident and reflected waves from port 1 and port 2, respectively. The scattering parameters are then known to satisfy the frequency-domain relation

$$b_1 = \tilde{S}_{11} a_1 + \tilde{S}_{12} a_2 \tag{6}$$

$$b_2 = \tilde{S}_{21} a_1 + \tilde{S}_{22} a_2. \tag{7}$$

$\tilde{S}_{11}$ and $\tilde{S}_{22}$ are regarded as scattering reflection coefficients, whereas $\tilde{S}_{12}$ and $\tilde{S}_{21}$ are the scattering transmission coefficients of the network. The total voltages in ports 1 and 2 are, respectively, given by

$$V_1 = a_1 + b_1 \tag{8}$$

$$V_2 = a_2 + b_2 \tag{9}$$

and the expressions for the currents are

$$I_1 = \frac{a_1}{Z_{\text{ref}}} - \frac{b_1}{Z_{\text{ref}}} \tag{10}$$

$$I_2 = \frac{a_2}{Z_{\text{ref}}} - \frac{b_2}{Z_{\text{ref}}}. \tag{11}$$

A relation between the propagation characteristics of a transmission line and the associated scattering parameters can then be easily derived. For a single mode of propagation, it can be shown that for a given transmission line

$$\tilde{S}_{11} = \tilde{S}_{22} = \frac{(1-\alpha^2)\rho}{1-\rho^2\alpha^2} \qquad \tilde{S}_{12} = \tilde{S}_{21} = \frac{(1-\rho^2)\alpha}{1-\rho^2\alpha^2} \tag{12}$$

$$\alpha = e^{-\gamma l} \qquad \rho = \frac{Z_0(\omega) - Z_{\text{ref}}}{Z_0(\omega) + Z_{\text{ref}}} \tag{13}$$

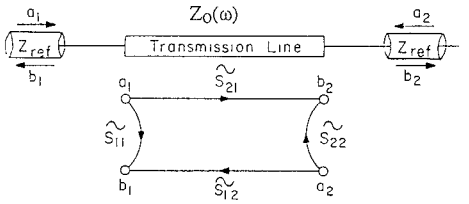

Fig. 2. Transmission line and frequency-domain flow-graph representation using scattering parameters.

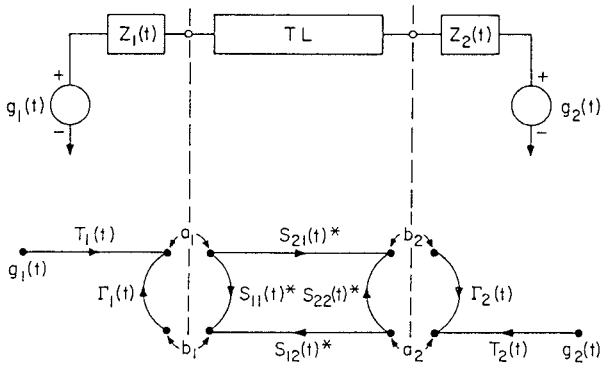

Fig. 3. Time-domain circuit and flow-graph representation of arbitrary transmission line (TL) with nonlinear terminations at time t. The sign * indicates a convolution between time-domain scattering parameters and the independent voltage waves a_1 and a_2 as per (14) and (15).

where $\alpha(\omega)$ and $Z_0(\omega)$ account for the dispersive and lossy behaviors of the line. $Z_0(\omega)$ is the characteristic impedance of the line to be analyzed and must be distinguished from Z_{ref}, the characteristic impedance of the reference lines which support the voltage waves associated with the S parameters. The scattering parameters of a transmission line depend only on its electrical characteristics and are not influenced by the source and load voltages at the terminations; however, the overall response of the system is a combination of line and termination responses and can be obtained by cascading the various sections of the network. We can then write the time-domain equations relating the voltage waves of an arbitrary line terminated with nonlinear loads (Fig. 3). We get (subscripts 1 and 2 refer to near end and far end, respectively)

$$b_1(t) = S_{11}(t)*a_1(t) + S_{12}(t)*a_2(t) \tag{14}$$

$$b_2(t) = S_{21}(t)*a_1(t) + S_{22}(t)*a_2(t) \tag{15}$$

where * indicates a convolution in the time domain. The scattering parameters $S_{11}(t), S_{12}(t), S_{21}(t), S_{22}(t)$ are the inverse transforms of the frequency-domain S parameters and can be viewed as Green's functions associated with the time-domain response of the transmission line, due to a single frequency source at the terminations. The load conditions at the near and far ends are now directly expressed in the time domain by looking at the flow-graph representation of the system (see Fig. 3)

$$a_1(t) = \Gamma_1(t)b_1(t) + T_1(t)g_1(t) \tag{16}$$

$$a_2(t) = \Gamma_2(t)b_2(t) + T_2(t)g_2(t) \tag{17}$$

in which $\Gamma_1(t), \Gamma_2(t), T_1(t), T_2(t)$ are the reflection and transmission coefficients associated with near and far ends, respectively:

$$T_i(t) = \frac{Z_{ref}}{Z_i(t) + Z_{ref}} \qquad \Gamma_i(t) = \frac{Z_i(t) - Z_{ref}}{Z_i(t) + Z_{ref}} \tag{18}$$

In (14) and (15), each of the convolution terms can be expressed as

$$S_{ij}*a_j = \int_0^t S_{ij}(t-\tau)\,a_j(\tau)\,d\tau. \tag{19}$$

Since the algorithm to be derived must be amenable to computer usage, it is desirable to discretize (19) and isolate $a_j(t)$ in a manner analogous to [11, eqs. (12) and (13)]:

$$S_{ij}(t)*a_j(t) = \sum_{\tau=1}^{t} S_{ij}(t-\tau)\,a_j(\tau)\,\Delta\tau$$

$$S_{ij}(t)*a_j(t) = S_{ij}(0)\,a_j(t)\Delta\tau + \sum_{\tau=1}^{t-1} S_{ij}(t-\tau)\,a_j(\tau)\Delta\tau \tag{20}$$

or

$$S_{ij}(t)*a_j(t) = S'_{ij}(0)\,a_j(t) + H_{ij}(t) \tag{21}$$

where $\Delta\tau$ is the time step and $S'_{ij}(0) = S_{ij}(0)\Delta\tau$. $H_{ij}(t) = \sum_{\tau=1}^{t-1} S_{ij}(t-\tau)\,a_j(\tau)\Delta\tau$ represents the history of the line and depends on information up to time $t-1$. Causality insures that the a_j's are known for $\tau < t$, which allows the use of this information for the determination of the a_j's at $\tau = t$. We first substitute (21) into (14) and (15) and obtain

$$b_1(t) = S'_{11}(0)\,a_1(t) + S'_{12}(0)\,a_2(t) + H_{11}(t) + H_{12}(t) \tag{22}$$

$$b_2(t) = S'_{21}(0)\,a_1(t) + S'_{22}(0)\,a_2(t) + H_{21}(t) + H_{22}(t). \tag{23}$$

Combining the above equations with those for the forward waves (16) and (17), one gets

$$a_1(t) = \frac{[1 - \Gamma_2(t)S'_{22}(0)][T_1(t)g_1(t) + \Gamma_1(t)M_1(t)]}{\Delta(t)} + \frac{\Gamma_1(t)S'_{12}(0)[T_2(t)g_2(t) + \Gamma_2(t)M_2(t)]}{\Delta(t)} \tag{24}$$

$$a_2(t) = \frac{[1 - \Gamma_1(t)S'_{11}(0)][T_2(t)g_2(t) + \Gamma_2(t)M_2(t)]}{\Delta(t)} + \frac{\Gamma_2(t)S'_{21}(0)[T_1(t)g_1(t) + \Gamma_1(t)M_1(t)]}{\Delta(t)} \tag{25}$$

$$\Delta(t) = [1 - \Gamma_1(t)S'_{11}(0)][1 - \Gamma_2 S'_{22}(0)] - \Gamma_1(t)S'_{12}(0)\Gamma_2(t)S'_{21}(0) \tag{26}$$

where $M_1(t) = H_{11}(t) + H_{12}(t)$, and $M_2(t) = H_{21}(t) + H_{22}(t)$. The variables $b_1(t)$ and $b_2(t)$ are recovered using (22) and (23), and the total voltages at ports 1 and 2, by using (8) and (9). Fig. 4 shows the flow-graph representation for the transmission line at time t in which the memory of the complete network has been included in the terms $M_1(t)$ and $M_2(t)$. The independent terms are $g_1(t)$

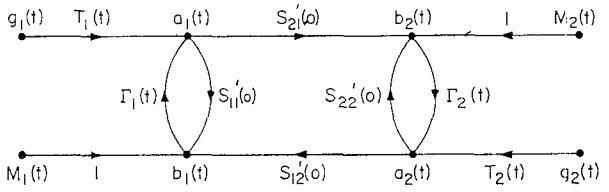

Fig. 4. Equivalent flow-graph representation of arbitrary transmission line with nonlinear time-varying terminations at time t. The history of the network is included via the memory variables $M_1(t)$ and $M_2(t)$. Note that this representation involves only multiplications in the time domain.

and $g_2(t)$. $M_1(t)$ and $M_2(t)$ are also independent and contain the information pertinent to the history of the line. Numerical efficiency is of practical importance for the simulation since it determines the speed of the computations involved. Expressions (24)–(26) can be further reduced by observing that for transmission lines with nonzero length, $S'_{12}(0)$ and $S'_{21}(0)$ must vanish, since a finite duration is required for an arbitrary signal to propagate through the line. The above relations then become

$$a_1(t) = \frac{[1-\Gamma_2(t)S'_{22}(0)][T_1(t)g_1(t)+\Gamma_1(t)M_1(t)]}{\Delta(t)} \tag{27a}$$

$$a_2(t) = \frac{[1-\Gamma_1(t)S'_{11}(0)][T_2(t)g_2(t)+\Gamma_2(t)M_2(t)]}{\Delta(t)} \tag{27b}$$

$$b_1(t) = S'_{11}(0)a_1(t)+M_1(t) \tag{27c}$$

$$b_2(t) = S'_{22}(0)a_2(t)+M_2(t) \tag{27d}$$

with

$$\Delta(t) = [1-\Gamma_1(t)S'_{11}(0)][1-\Gamma_2(t)S'_{22}(0)]. \tag{28}$$

Computational limitations in these expressions are essentially determined by $M_1(t)$ and $M_2(t)$, which contain the history of the network and involve the voltage wave solutions from previous time steps. In the case where losses and dispersion are neglected, the frequency-domain scattering parameters associated with the transmission line become

$$\tilde{S}_{11}(\omega) = \tilde{S}_{22}(\omega) = \frac{(1-e^{-2j\omega l/v})\rho}{1-\rho^2 e^{-2j\omega l/v}} \tag{29}$$

$$\tilde{S}_{12}(\omega) = \tilde{S}_{21}(\omega) = \frac{(1-\rho^2)e^{-j\omega l/v}}{1-\rho^2 e^{-2j\omega l/v}} \tag{30}$$

where

$$\rho = \frac{Z_0 - Z_{\text{ref}}}{Z_0 + Z_{\text{ref}}}. \tag{31}$$

Since Z_0, the characteristic impedance of the line, is constant with time, and since Z_{ref}, the reference impedance, is arbitrary, one can choose $Z_{\text{ref}} = Z_0$, which leads to $\rho = 0$ and

$$\tilde{S}_{11}(\omega) = \tilde{S}_{22}(\omega) = 0 \tag{32}$$

$$\tilde{S}_{12}(\omega) = S_{21}(\omega) = e^{-j\omega l/v}. \tag{33}$$

Therefore, the time-domain Green's functions associated with the scattering parameters are

$$S_{11}(t) = S_{22}(t) = 0 \tag{34}$$

$$S_{12}(t) = S_{21}(t) = \delta\left(t - \frac{l}{v}\right) \tag{35}$$

$$M_1(t) = a_2(t - l/v) \tag{36}$$

$$M_2(t) = a_1(t - l/v) \tag{37}$$

$$\Delta(t) = 1. \tag{38}$$

We then obtain simple expressions for the forward and backward waves:

$$a_1(t) = T_1(t)g_1(t)+\Gamma_1(t)a_2(t - l/v) \tag{39}$$

$$a_2(t) = T_2(t)g_2(t)+\Gamma_2(t)a_1(t - l/v) \tag{40}$$

$$b_1(t) = a_2(t - l/v) \tag{41}$$

$$b_2(t) = a_1(t - l/v). \tag{42}$$

The advantage of the above expressions lies in their computational efficiency, since only a search is involved in the evaluation of the history of the network, and no summations of previously calculated terms are needed.

IV. Models for Terminations and Devices

Thus far, this study concentrated on simulating the time-domain transient response for arbitrary transmission lines terminated with nonlinear devices. In this section, we examine the nature of the terminations and the manner in which they are to be represented in a form consistent with the relations derived. Several techniques are available that convert reactive elements and nonlinear devices to time-varying causal resistances as well as voltage or current sources. We briefly overview two of these techniques, namely, the trapezoidal algorithm and the Newton–Raphson (NR) algorithm. A more detailed development can be found in [15]. Since formulation and solution are in the time domain, every element must have an equivalent network in the time domain. The trapezoidal algorithm is a numerical integration algorithm, and its use in representing reactive elements in the time domain is illustrated below. Consider a capacitor C, with a current–voltage relation given by

$$I = C\frac{dV}{dt}. \tag{43}$$

If we discretize the time variable by choosing a time step h, then the voltage V_{n+1} at time $t_{n+1} = (n+1)h$ can be approximated in terms of variables at $t = nh$ as

$$V_{n+1} = V_n + \frac{h}{2}V'_{n+1} + \frac{h}{2}V'_n \tag{44}$$

where the superscript $'$ indicates a derivative with respect to time. Making use of (43), we get

$$I_{n+1} = \frac{2C}{h}V_{n+1} - \left(\frac{C}{h}V_n + i_n\right). \tag{45}$$

Equation (45) can then be represented by the equivalent

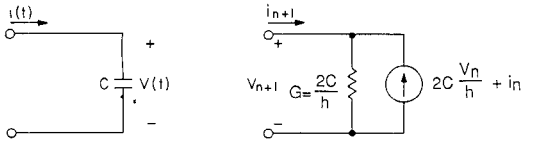

Fig. 5. Linear capacitor and equivalent time-domain trapezoidal algorithm representation.

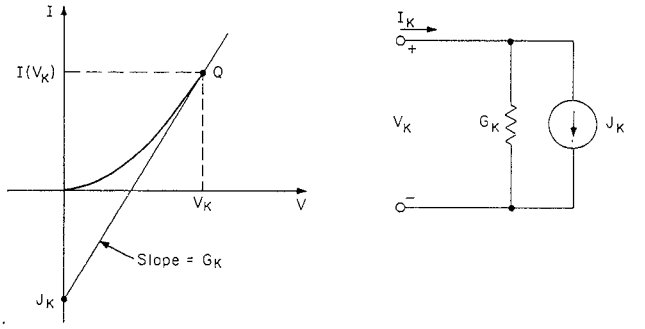

Fig. 6. Geometrical and circuit interpretation of the Newton–Raphson algorithm at the kth iteration.

linear one-port model at time $t_{n+1}=(n+1)h$ (see Fig. 5) with conductance $G=\frac{2C}{h}$ and current source $J_n=\frac{2C}{h}V_n+i_n$. An analogous derivation can be performed for inductances as well. The efficiency of the method depends on a proper choice of the time step which determines the stability of the numerical solution. Several other techniques of numerical integration are also available which offer greater stability at the price of numerical complexity [15].

Nonlinear elements such as diodes and transistors must be reduced to equivalent networks with linear elements at time t. If the nonlinear current voltage relation for these elements is known, then an iterative scheme such as the Newton–Raphson algorithm can be used to seek a solution. The circuit representation of the Newton–Raphson technique is illustrated in Fig. 6. At a particular time, a guess value for the voltage is chosen to which a current is associated via the $I-V$ relations that determine the operating point Q. The next guess is then related to the previous one by

$$V_{k+1}=V_k-\left[\frac{dI}{dV}\right]^{-1}I_k. \tag{46}$$

At each iteration step, the resulting equivalent circuit is composed of a linear conductance of value $G_k=dI/dV$ at V_k and a current source with value given by $J_k=I(V_k)-G_kV_k$. Solving the combined transmission line Newton–Raphson equivalent circuit problem at each iteration step will lead to the actual representation of the termination at time t.

Once linearization and discretization are performed, time-domain values are available for the equivalent resistances or generators. These expressions are causal, since their values at any time t depend on the history of the network which renders impossible an *a priori* knowledge of the time variations of the termination impedance. Nonlinear complex elements can be handled by first using the NR scheme for linearization at a given time, then stepping in the time domain while replacing linear complex elements by time-varying resistances and generators.

V. Applications and Practical Considerations

Many applications in microwave and digital communications require the use of transmission lines terminated with nonlinear devices. Distortion and noise arise when the terminations are not matched to the line impedance. Moreover, if losses and dispersion are present in the line, attenuation and time delay come into account. The combination of these effects needs to be modeled and simulated on a reliable computer-aided design (CAD) tool. Simulations of pulse propagation through lossy transmission lines terminated with active devices can be very useful in predicting signal distortion, attenuation, rise and fall time degradation which occur along the transmission path. The necessary information for such a tool are the line parameters over a wide frequency range and complete device characteristics. The line parameters can be found from a frequency-domain full-wave dispersion analysis which includes the effects of losses. Device data are usually obtained from the current–voltage characteristics provided by the manufacturers.

Several computer simulation programs were developed to simulate waveform distortion on various combinations of transmission lines and terminations. First, a lossless stripline structure terminated with advanced Schottky (AS) TTL inverters was studied (see Fig. 7). The length of the line was 50 in (1.27 m) with $Z_0=73\ \Omega$, $v=0.142$ m/ns. The line was excited by the output of an AS04 inverter (driver). The receiving end of the line was connected to the inputs of eight AS240 inverters. For computational efficiency, a simple dynamic nonlinear equivalent circuit was used to model the output of the driver. The network consisted of a voltage generator in series with a voltage-dependent resistor. An 8 pF capacitor was placed in parallel with the combination to model rise and fall time degradation and RC time delays (see Fig. 7(b)). The generator provided a pulse with a magnitude of 4.2 V. The voltage dependence of the resistance is shown in Fig. 7(b). The quick jump in resistance is used to model the cutoff point of one output transistor of the TTL inverter. The input of each AS240 inverter was modeled as a reverse-biased Schottky diode in parallel with an 8 pF capacitor (see Fig. 7(c)). The simulation process involved first choosing a time interval and then stepping in time and determining the voltage variables as per (39)–(42). The trapezoidal scheme was used to convert capacitors to linear sources and resistances. Likewise, the Newton–Raphson algorithm made it possible to convert the Schottky diodes into a linearized equivalent circuit. The time steps were found to have no significant effects on the accuracy of the solutions due to the good stability properties of the trapezoidal algorithm. Experimental results are compared with the simulations in Fig. 8(a) and (b). Minor discrepancies were attributed to pin and socket inductances, which were not accounted for in the model. Likewise, charge control ef-

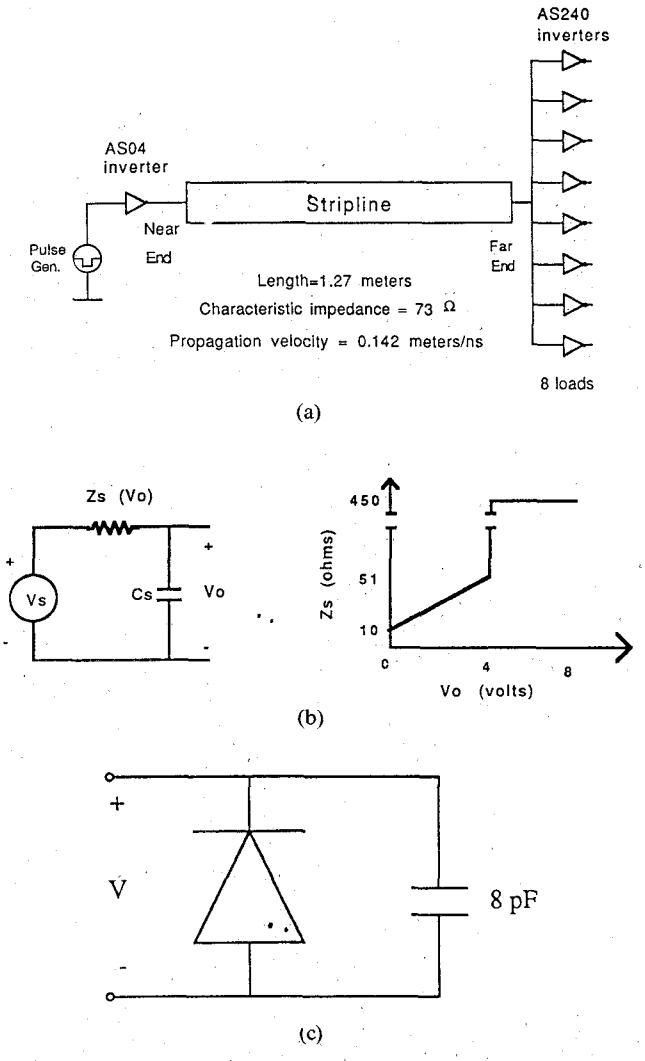

Fig. 7. (a) Configuration used for simulation of transients on a stripline structure with nonlinear loads. (b) Model used for AS04 driver with voltage dependence of impedance, $C_s = 8$ pF. $V_s(t)$ has the following characteristics: width = 108 ns, rise time = 5 ns, fall time = 4 ns. (c) Model used for the input of each AS240 receiver. The diode has a saturation current $I_s = 10^{-12}$ A.

fects, which determine rise and fall time degradation as well as time delay through the inverters, were not modeled. The otherwise overall good agreement indicated the validity of the simplified device models.

Losses were also analyzed using (27). First, the frequency-domain scattering parameters were calculated for the transmission line shown in Fig. 9. Skin effect in the conductor was accounted by a $\sqrt{f}$ behavior of the resistance per unit length. Once the frequency dependence of the scattering parameter was determined, a fast Fourier transform (FFT) algorithm was used to solve for the time-domain Green's functions associated with the S parameters. Then (20)–(28) were used to calculate the voltage waves. Fig. 9 shows the configuration used to predict and compare waveforms on lossless and lossy microstrip lines. The low-frequency characteristics of the line were: $L_0 = 539$ nH/m and $C_0 = 39$ pF/m. The resistance per unit length for the lossy case was $R_0 = \sqrt{f\ (\text{in GHz})}\ 1\ \text{k}\Omega/\text{m}$. Dielectric losses were neglected

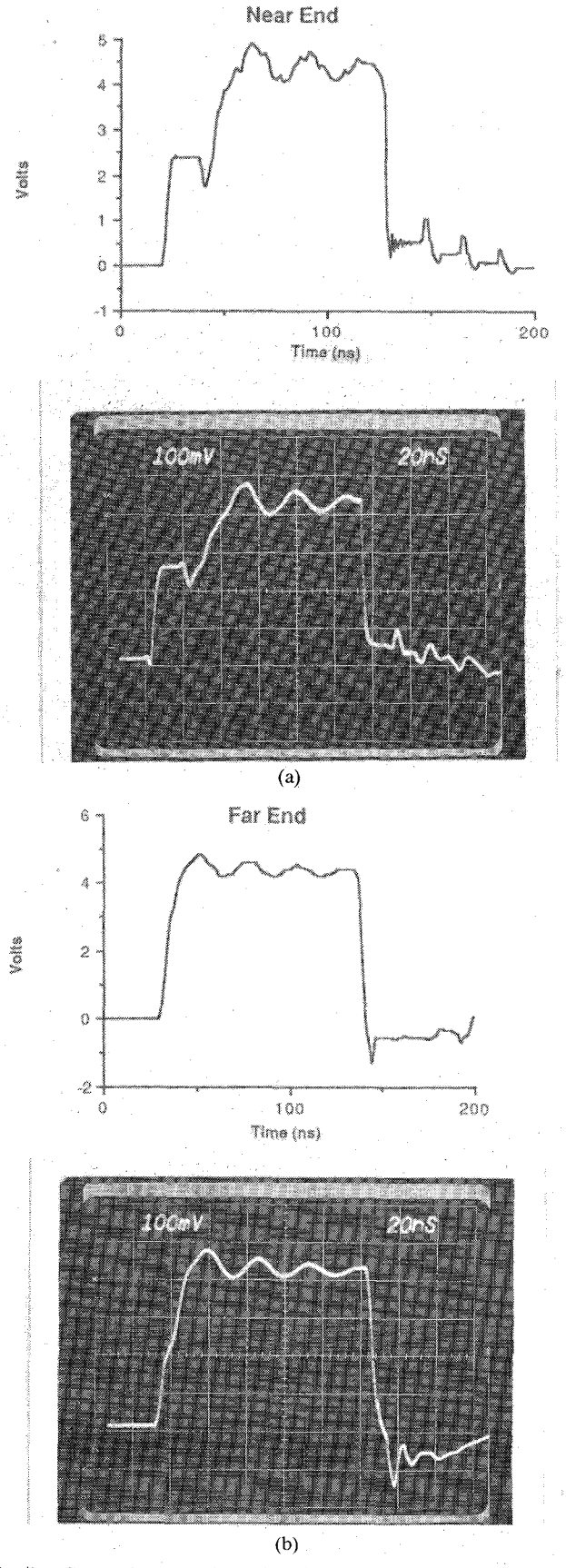

Fig. 8. Comparison of theoretical (plots) and experimental (photographs) simulations for the stripline structure terminated with AS inverters of Fig. 7 at (a) the near end and (b) the far end. Vertical scales in experimental simulations have a probe attenuation factor of 10.

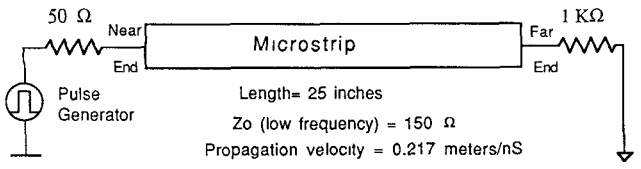

Fig. 9. Microstrip configuration used to simulate the effects of losses. Line length = 25 inches (0.635 meters). Low-frequency electrical characteristics: $L_0 = 539$ nH/m, $C_0 = 39$ pF/m. Loss characteristics: $R_0 = \sqrt{f}$ in GHz 1 kΩ/m and $G_0 = 0$ mhos/meter. Pulse characteristics: magnitude = 4 V, width = 20 ns, rise and fall times = 1 ns.

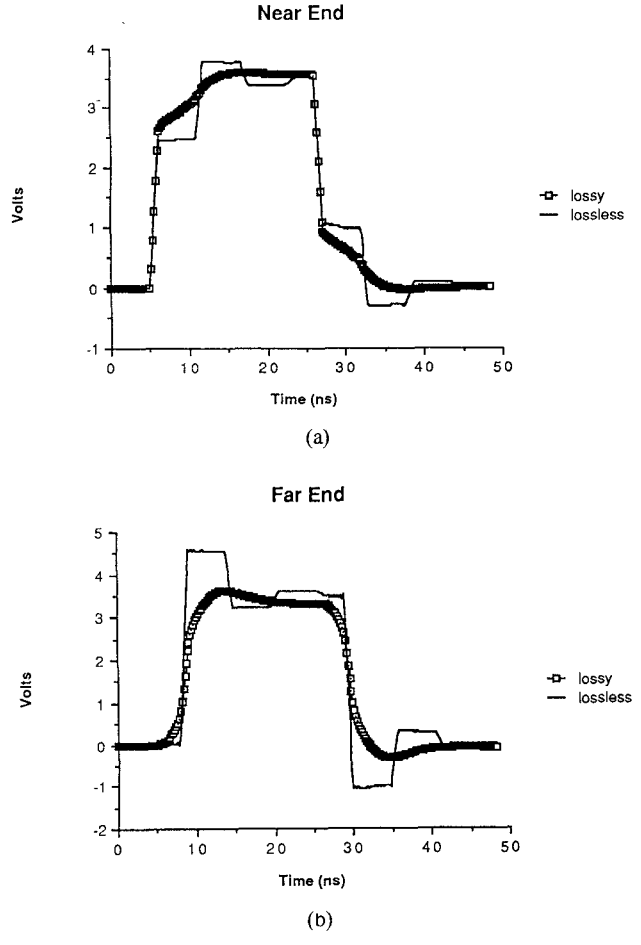

Fig. 10. Comparisons between responses for lossless and lossy cases for the microstrip structure of Fig. 9 at (a) the near end and (b) the far end.

($G_0 = 0$), which is a good representation of many interconnections in integrated circuit design. The above configuration was excited by a 4 V pulse generator with an internal impedance of 50 Ω, and a termination impedance of 1 kΩ. A comparison between lossy and lossless cases is shown in Fig. 10. As anticipated, the introduction of losses led to rise and fall time degradation and waveform attenuation. Experimental simulations were not available due to the lack of reliable measurement techniques for accurately determining the frequency dependence of microstrip loss parameters. Such information is essential in developing models to be used in conjunction with the simulations. Other alternatives would include providing a set of measured scattering parameters for an arbitrary (lossy and dispersive) transmission line over a wide frequency range (up to 18 GHz). Time-domain Green's functions can then be numerically computed and used to calculate the associated response.

VI. Conclusions

This study explored some important aspects of interconnections for digital and microwave applications. The problems of losses, dispersion, and load nonlinearities were analyzed. A simple algorithm was derived for the simulation of an arbitrary time-domain signal on a structure having all the above properties. The algorithm assumed that the frequency-dependent characteristics of the line were available as well as large-signal models for the terminations. Future work includes the derivation of a suitable loss and dispersion model and the extension of the algorithm for modeling n-line multiconductor systems.

References

[1] W. J. Getsinger, "Microstrip dispersion model," *IEEE Trans. Microwave Theory Tech.*, vol. MTT-21, pp. 34–39, Jan. 1973.

[2] W. J. Getsinger, "Measurement and modeling of the apparent characteristic impedance of microstrip," *IEEE Trans. Microwave Theory Tech.*, vol. MTT-31, pp. 624–632, Aug. 1983.

[3] P. Bhartia and P. Pramanick, "New microstrip dispersion model," *IEEE Trans. Microwave Theory Tech.*, vol. MTT-32, pp. 1379–1384, Oct. 1984.

[4] H. J. Carlin, "A simplified circuit model for microstrip," *IEEE Trans. Microwave Theory Tech.*, vol. MTT-21, pp. 589–591, Sept. 1973.

[5] E. J. Denlinger, "A frequency dependent solution for microstrip transmission lines," *IEEE Trans. Microwave Theory Tech.*, vol. MTT, pp. 30–39, Jan. 1971.

[6] T. Itoh and R. Mittra, "Spectral-domain approach for calculating the dispersion characteristics of microstrip lines," *IEEE Trans. Microwave Theory Tech.*, vol. MTT-21, pp. 496–499, July 1973.

[7] R. Mittra and T. Itoh, "New technique for the analysis of the dispersion characteristics of microstrip lines," *IEEE Trans. Microwave Theory Tech.*, vol. MTT-19, pp. 47–56, Jan. 1971.

[8] E. F. Kuester and D. C. Chang, "Theory of dispersion in microstrip of arbitrary width," *IEEE Trans. Microwave Theory Tech.*, vol. MTT-28, pp. 259–265, Mar. 1980.

[9] M. Hashimoto, "A rigorous solution for dispersive microstrip," *IEEE Trans. Microwave Theory Tech.*, vol. MTT-33, pp. 1131–1137, Nov. 1985.

[10] T. C. Edwards and R. P. Owens, "2–18 GHz dispersion measurement on 10–100 Ω microstrip lines on sapphire," *IEEE Trans. Microwave Theory Tech.*, vol. MTT-24, pp. 506–513, Aug 1976.

[11] A. R. Djordjevic, T. K. Sarkar, and R. F. Harrington, "Analysis of transmission lines with arbitrary nonlinear terminal networks," *IEEE Trans. Microwave Theory Tech.*, vol. MTT-21, pp. 660–666 June 1986.

[12] H. Mohammadian and C. T. Tai, "A general method of transient analysis for lossless transmission lines and its analytical solution to time-varying resistive terminations," *IEEE Trans. Antennas Propagat.*, vol. AP-32 pp. 309–312, Mar. 1984.

[13] R. L. Veghte and C. A. Balanis, "Dispersion of transient signals in microstrip transmission lines," *IEEE Trans. Microwave Theory Tech.*, vol. MTT-34, pp. 1427–1436, Dec. 1986.

[14] S Caniggia, "EMC design of digital systems using macromodeling procedures for integrated circuits and their interconnections," in *Proc. EMC Symp.*, 1983, pp. 465–470.

[15] L. O. Chua and P. M. Lin, *Computer-Aided Analysis of Electronic Circuits*. Englewood Cliffs, NJ: Prentice Hall, 1975.

[16] D. K. Ferry, J. M. Golio, and R. O. Grondin, "Interconnections and limitations in VLSI," in *Proc. VLSI Multilevel Interconnection Conf.*, 1985, pp. 408–415.

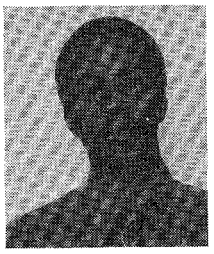

Jose E. Schutt-Aine (S'87) was born in Petion-Ville, Haiti, on October 25, 1959. He received the B.S. degree in electrical engineering from the Massachusetts Institute of Technology, Cambridge, in 1981. From 1981 to 1983, he worked at the Hewlett-Packard Technology Center in Santa Rosa, CA. He received the M.S. degree in electrical engineering from the University of Illinois, Urbana, in 1984 and is currently pursuing the Ph.D. degree at the same institution.

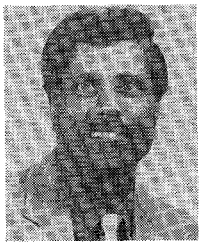

Raj Mittra (S'54–M'57–SM'69–F'71) is the Director of the Electromagnetic Communication Laboratory of the Electrical and Computer Engineering Department and Research Professor of the Coordinated Science Laboratory at the University of Illinois. He is a Past-President of the IEEE Antennas and Propagation Society. He serves as a consultant to several industrial and governmental organizations in the United States.

His professional interests include the areas of analytical and computer-aided electromagnetics, high-speed digital circuits, radar scattering, satellite antennas, microwave and millimeter-wave integrated circuits, frequency selective surfaces, EMP and EMC analysis, and the interaction of electromagnetic waves with biological media.